Lasers in the Conservation of Artworks XIII – Siano & Ciofini (eds)

Evaluation of femtosecond laser texturing on carbonate heritage stones

A.J. López Díaz & A. Ramil
Laboratorio de Aplicacións Industriais do Láser, Campus Industrial de Ferrol, Universidade da Coruña, Ferrol, Spain

D.M. Freire-Lista
Universidade de Trás-os-Montes e Alto Douro, UTAD, Escola de Ciências da Vida e do Ambiente, Quinta dos Prados, Vila Real, Portugal
Centro de Geociências, Universidade de Coimbra

ABSTRACT: The effect of femtosecond laser texturing on Carrara marble, Montesclaros marble, and Redueña dolostone was evaluated. Mineralogical characterisation, laser structuring of thin sections and hand samples of the three heritage stones were carried out. The topography of the textured surfaces was obtained by means of interferometric microscopy, and a petrographic study of laser-generated craters in thin sections was performed to elucidate the effect of the crystalline structure of calcite on the morphology of the laser-generated structures. The differences observed in thin sections allowed to understand the differences observed in laser-structured bulk samples of the three heritage stones; which is key aspect when designing conservative strategies based on laser texturing.

1 INTRODUCTION

Carbonaceous stones have been used in the carving of sculptures throughout history (Cassar 2010, Freire-Lista 2021). The availability of these stones, particularly marble and dolostone, determined their widespread use. These building stones are found in much of the world's heritage, thanks primarily to its purity, homogeneity, colour, and polishability (Siegesmund et al. 2000). In addition, dolomite has been chosen as building stone for fountains due to lower solubility than marble (Freire-Lista & Fort 2017, 2019).

Paseo del Prado of Madrid (Spain) was promoted by King Carlos III in the 18th century. It has three aligned fountains: Cibeles at the northern end; Apollo (or Four Seasons), in the centre; and Neptuno, at the southern end. Cibeles and Neptuno Fountains are built mainly with Montesclaros marble and Apollo Fountain is built with Redueña dolomite (Freire-Lista 2020). Prado-Retiro axis was declared a UNESCO World Heritage Site in 2021 and it is one of the most touristic areas of Spain. The conservation of this urban heritage is a challenging task; it is conducted through a multiplicity of both theoretical and methodological perspectives that require an interdisciplinary vision (De Wever et al. 2017; Huerta-Murillo et al. 2019; Salvini et al. 2022).

Hydrophobic protective treatments, which decrease the water ingress in the stone surface, being developed. In this sense, chemicals with varying degrees of toxicity are often applied to create a surface layer. Laser texturing, both in nanosecond (ns) and femtosecond (fs) pulses, currently used in different industrial and technological fields has been investigated as an environmentally friendly alternative to reduce the wettability of stones (Fiorucci et al. 2014, Pou-Álvarez et al. 2021). Laser texturing of marble has resulted in an increase in the contact angle

DOI: 10.1201/9781003386872-25

above 90º, giving the surface a hydrophobic, and even superhydrophobic, character (Ariza et al. 2022, Carrascosa et al. 2022, López et al. 2019); however, in other stones such as slate, quartzite or granite, laser texturing caused a decrease in the contact angle, thus increasing the hydrophilic nature of the surface (López et al. 2022). These results highlight the need further research on laser texturing in natural stones; given that the challenge is their heterogeneity that causes different interaction mechanisms of the laser pulses with each type of grain, leading to irregular surface absorption. Moreover, the petrographic properties of heritage stones largely condition their durability and forms of deterioration (Fehér & Török 2022; Martínez-Martínez et al 2011; Weber et al. 2011), and thus, it is necessary a petrographic study of the laser-generated structures in thin sections, not only in bulk samples, owing that this knowledge is essential to know the morphology of the ablated area in each of the constituent minerals of heritage stones.

The aim of this study is to assess, at the petrographic microscope scale, the effect of femtosecond laser texturing of the calcareous heritage stones used in the main fountains of Paseo del Prado (Madrid, Spain); that is: Carrara marble (CM), Montesclaros marble (MM) and Redueña Dolostone (RD). The methods used, and data obtained are useful for heritage conservation purposes. The femtosecond laser effect in each calcareous stone allows to solve the problem of the lack of information about the response to the femtosecond laser of each of the mineralogical textures present in different carbonate stones used in the Prado-Retiro axis UNESCO World Heritage Site 2021, and to establish a conservation and restoration plan (Salvini et al 2023).

2 MATERIALS AND METHODS

2.1 *Carrara Marble (CM)*

CM was used since pre-historic times and found in many Roman patrician structures such as the Pantheon at Agrippa and Trajan's Column, it was exported from the port at Luni to the entire Roman Empire. CM, specifically 'Statuario Michelangelo' marble is quarried at Monte Altissimo in the Apuan Alps around Carrara, Tuscany (Italy) (44 0300800 N, 10 1400400 E). It bellows to the Apuane Unit, the lowermost of the Tuscan units. This marble is characterised by a uniform composition and colour (white, locally streaked with thin brownish veins and dark sub-millimetric laminates) and exhibited no cracking visible to the naked eye (Murru et al. 2028). The two putti located at the back of the carriage of Cibeles Fountain are carved in this marble (López de Azcona et al. 2002).

2.2 *Montesclaros Marble (MM)*

MM outcrops in the Gredos Complex, in a band approximately 11 km long and up to 1 km wide, between the villages of Hontanares and Montesclaros, where these are high grade regional metamorphic materials. MM is quarried approximately 140 km from Madrid and approximately 15 km north of Talavera de la Reina (Toledo, Spain). It is predominantly white, white-bluish in colour. In addition, there are grey, blue grey, cream, pink and cream marbles. This dolomitic marble has crystals visible to the naked eye. The fountains of Cibeles and Neptuno are built with this marble (Freire-Lista 2020).

2.3 *Redueña Dolostone (RD)*

Due to difficulties in financing of CM for the fountains, the architect Ventura Rodríguez proposed the use of Redueña dolostone (RD) for the construction of Apollo fountain. Redueña stone includes limestone and dolomicrites, normally of cream colour tones. Its historical quarries were very dispersed, notably the villages of Redueña, Guadalix de la Sierra, El Molar, Venturada and Torrelaguna, as well as other towns in Guadalajara, Spain (Fort et al. 2013, Sanz et al. 2015). The dolostone correspond to the Montejo member that forms part of the

Castrojimeno Formation (Santonian). This member has a level of Trochactaeon Lamarcki specie gastropods and it outcrops in the around Redueña Village (Freire-Lista & Fort 2017). This member has been used for the construction of Apollo fountain, in the Paseo del Prado of Madrid and it is the one that has been tested in this work.

2.4 *Sampling*

Samples of CM are of 'Statuario Michelangelo' marble, a variety quarried at Monte Altissimo in the Apuan Alps around Carrara, Tuscany (Italy), in the quarry located at the coordinates: 44.05183618, 10.24049532. Samples of MD were extracted from a historical quarry at Montesclaros (40.078169, -4.933098). Samples of RD (Castrojimeno Formation) was extracted from Redueña village, located approximately 50 km North of Madrid, in a historical quarry located at the coordinates 40.80208, -3.59141.

All samples were cut and polished to make cuboids of 2 cm× 5 cm× 5 cm (bulk samples) and thin sections (2 cm × 3 cm × 30 μm). After cutting samples with a low speed saw, they were polished with sandpaper and progressively smaller diameter size of diamond spray (from 6, 3 to 1 μm of grain diameter) to get polished thin sections. The thin sections were observed under a Leica DM4500 P polarisation microscope, equipped with a digital FireWire Camera Leica DFC 290 HD that worked with the Leica application suite software LAS 4. To understand the effect of laser texturing, two micromosaics (parallel and crossed Nicols) were made with more than 200 microscopic images each, covering an approximate area of 4 cm^2. To facilitate the understanding of the results, a colour code has been established, assigning blue to CM, green to MM, and yellow to RD.

2.5 *Laser texturing*

The laser used was the Spirit system from Spectra Physics with emission wavelength 1040 nm and pulse width < 400 fs. The intensity profile at the laser output was near- Gaussian (M2 < 1.2) and the beam diameter at the exit of the laser head was 1.5 mm. The laser beam presents horizontal polarization (> 100:1). Pulse rate can be selected from single shot to 1 MHz, with maximum pulse energy of 40 μJ at 100 kHz. The maximum mean power output is > 4 W. A two-mirror galvanometric scanner (Raylase SuperscanIII-15) was used and scanned the laser beam in X-Y directions. The beam was focused by means of a F-theta objective lens, 160 mm focal length, up to a diameter of 30 μm. At the working plane, the beam polarisation was parallel to Y direction. All the processing experiments were performed in ambient air and off-line control of the ablation process was accomplished by optical microscopy (Nikon Eclipse L150) and digital image processing software.

Once the most suitable laser parameters for each stone were selected, structuring patterns were generated on both thin sections and bulk samples. In the case of thin sections, 20 horizontal series of craters 200 μm apart were made as it is shown in Figure 1; the number of laser shots per crater was increased from 1 shot (bottom) to 20 shots (top). In bulk samples, two types of texturing patterns were used; a matrix of holes and parallel grooves, and 40 μm, 60 μm and 80 μm separation between holes or grooves.

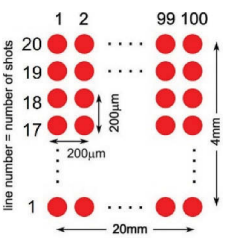

Figure 1. Scheme of laser texturing on the three thin sections (MM, CM and RD).

2.6 *Surface roughness*

A scanning white light interferometer (SWLI) microscope Zygo NewView 600 mounted in a vibration isolation table was used to evaluate the results of the texturing process. The vertical scan range was 150 μm with a vertical resolution of 0.1 nm. The image resolution was 640 × 480 pixels that gives a field view of 349.1 μm × 261.9 μm.

Data processing, analysis and visualisation were implemented by using Scientific Phyton. The same equipment was used to characterise the surface roughness of laser processed bulk samples in accordance with standard UNI-EN ISO 25178–2 (Int. Org. Standardization 2012).

3 RESULTS AND DISCUSSION

3.1 *Petrography of thin section mosaics*

Each carbonate stone has a different petrography. Figure 2 shows the mosaics of the texturing of the three thin sections (CM, MM and RD) using both parallel Nicols (a, b, c) and crossed Nicols (a', b', c'). The different colours of calcite crystals in Figures 2a', 2b', and 2c' indicate different crystallographic orientations. The extinction angle of calcite is symmetric or inclined with respect to the exfoliation traces.

CM is equigranular monocrystalline (Calcite), with a mean crystal size of 300 μm. Lamellar twins of calcite are common under {01-12}, and single twins are common under {0001}. Some crystals show perfect (rhombohedral) cleavage at {10-11}. The edges of the crystals are often straight. Intercrystallite microcracks border the edges of calcite crystals (Figure 2a). Rhombohedral exfoliation in the calcite contributed to the formation of normally straight intracrystalline microcracks.

MM is very coarse to coarse-grained (crystal size up to 5 mm) and it has granoblastic texture. The crystal boundaries are very sinuous, although few straight intercrystalline fractures are observed (Figures 2b and 2b').

RD is a massive dolostone, formed by micritic cement (particles ranging in diameter up to 4 μm formed by the recrystallisation of lime mud) with few mottled colours and poikilotopic and blocky mosaic cements predominate. RD has fossils filled with randomly oriented calcite that can reach sizes of 1 mm. The fossils are mainly composed of gastropods and fragments of bivalves. These fossils are found as molds filled with calcite crystals. The thickness of their shells can reach 3 mm thick. Remnants of their original depositional texture are preserved, generally disposed fossils aligned longitudinally to the lamination with few mottled colours and poikilotopic, and blocky mosaic cements predominate (Figures 2c and 2c').

An increase in diameter of the holes in relation to the number of laser shots delivered is appreciated in Figure 2. In this way, CM shows complete lines of craters perceptible under an optical microscope starting from shot number 6 (Figure 2a).

MM shows complete lines of craters perceptible from shot number 1 (Figure 2b). In case of RD thin section, different behaviour can be seen depending on the laser irradiated material; micritic cement shows complete lines of craters starting at line number 10 and recrystallized calcite shows craters at line 1.

Figure 3 depicts a scope of the areas highlighted in Figure 2, which allow us to observe the morphology of the laser generated structures: The craters on CM present an irregular morphology and, conversely, craters on MM present the most circular and regular morphology; with regards to RD, the morphology of the craters depends on the mineralogy on which the laser strikes. Differences in morphology can be intuited depending on the crystallographic direction of the calcite crystal on which the laser is incident. In this way, RD1 presents rectilinear fractures bordering the craters, while RD3 presents a rectangular morphology with the characteristic angles of the calcite structure. When the laser hits the micritic cement, the craters are more diffuse, maintaining a pseudo-circular morphology.

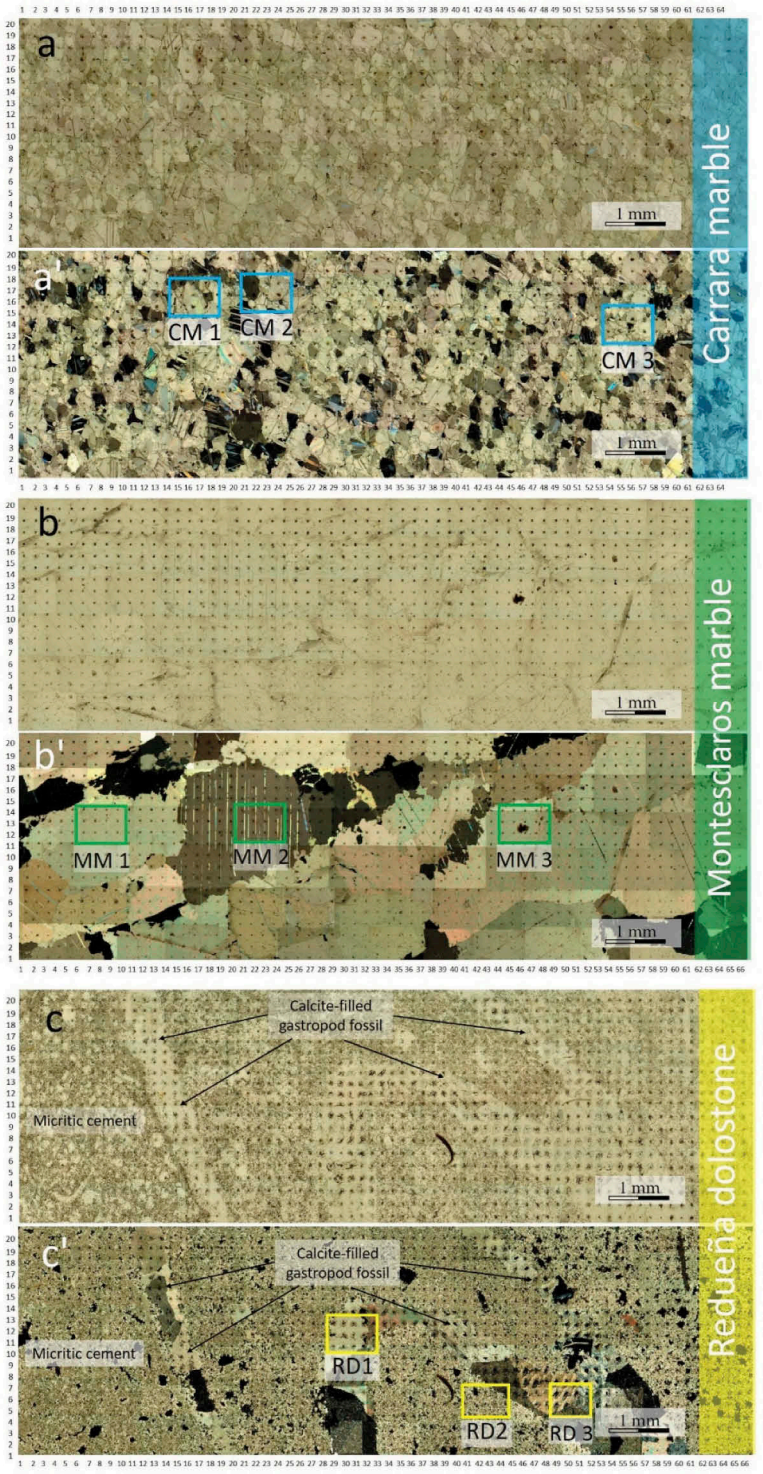

Figure 2. Petrographic mosaics of laser textured thin sections of Carrara marble (CM), Montesclaros marble (MM) and Redueña dolomite (RD).

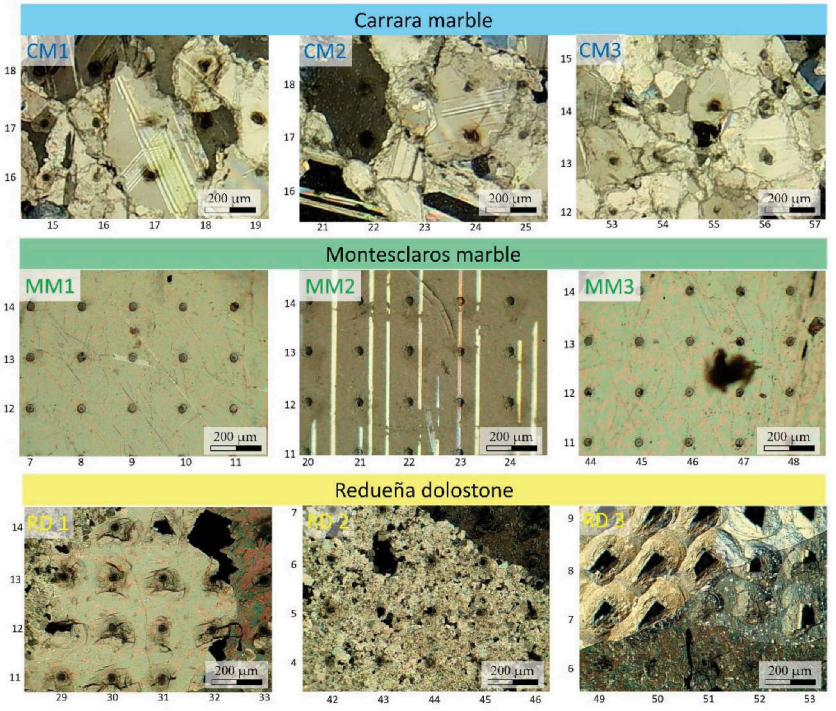

Figure 3. Enlargement of the rectangles indicated in the thin sections of Figure 2. Craters produced by laser texturing in Carrara marble (CM), Montesclaros marble (MM) and Redueña dolomite (RD) are shown in more detail.

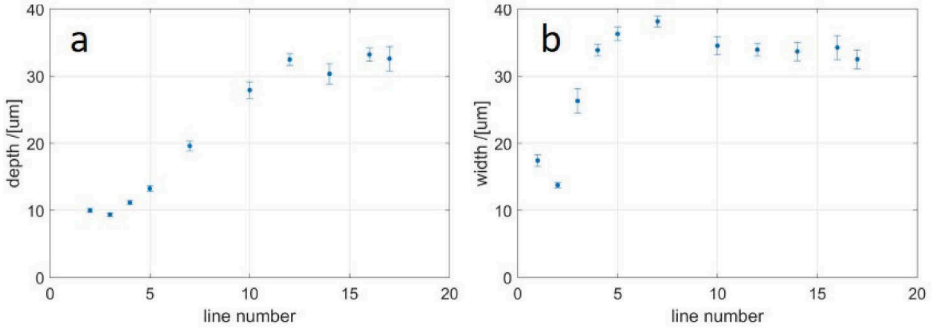

Figure 4. Crater size (µm) produced by laser texturing in Redueña Dolomite (RD) thin section as a function of the number of laser shots: a) depth, b) width.

3.2 *Thin section craters: Depth and width*

Topographies, obtained by fitting crater profiles to Gaussian bidimensional curves, allowed us to obtain the geometric parameters (depth and width) of the laser-generated structures. Figure 4 illustrates the dependence of the hole depth and width, on the number of laser shots in RD. Values were calculated by averaging 20 holes in each line.

In case of depth, Figure 4a), after the first five laser shots the dependence is nicely linear up to approximately 10-11 laser shots where saturation occurs for a hole depth of 30 µm.

This behaviour is similar in CM and MM marbles, though the saturation depth is lower than RD. Regarding width, a rapid increase is observed for the first five laser shots up to saturation that occurs for a hole width of 35 μm, as it was been expected given the diameter of the laser beam.

Note that starting from line 10, the average depth and width values present a greater dispersion and in this area the laser affects both calcite and micritic cement crystals. On the other hand, the lines that cross more calcite are from 1 to 8, 13 and 14, and the craters of lines 5 and 7 have a greater average width than the craters from line 10 onwards (Figures 2 and 4).

3.3 *Bulk samples*

Bulk samples were laser structured with two different patterns, a matrix of holes and parallel grooves, with different separation between them, "pitch": 40 μm, 60 μm and 80 μm, respectively. Figure 5 shows the topographies of both patterns at 60 μm pitch.

Images of the textured samples of CM, MM and RD, show how the grooves change their dimensions in CM when they cross calcites with different orientation (Figure 6 CM2, red arrows). The edges of the grooves show triangular fractures (yellow arrows). Regarding the hole matrix in CM, hole sizes vary according to the orientation of the calcite (Figure 6 CM3). In relation to MM, it has a larger crystal size, and it shows a more homogeneous hole and groove size. The image of RD textured with grooves shows a less uniform appearance.

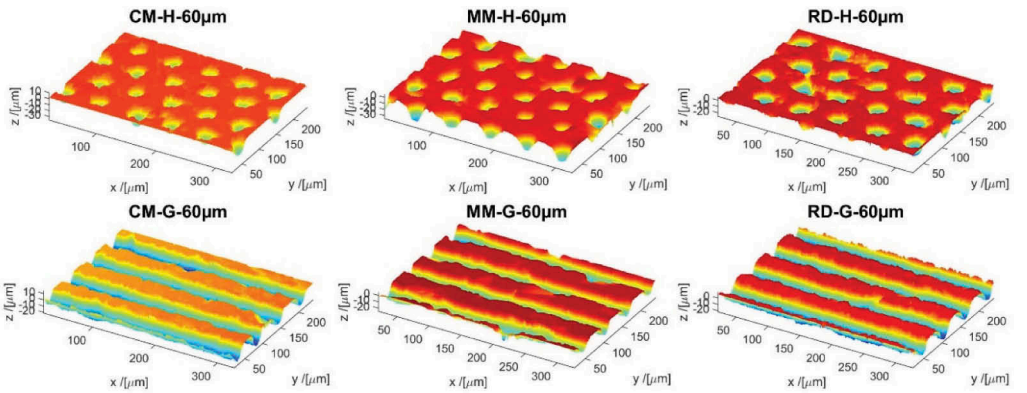

Figure 5. Topographies of the textured samples of Carrara marble (CM), Montesclaros marble (MM) and Redueña dolomite (RD). Texturing patterns are H (matrix of holes) and G (parallel grooves). Separation between structures 60 μm.

The areal roughness parameters of the textured surfaces were calculated from the topographies. Figure 7 depicts the values of the root mean square height, Sq, as a function of the "pitch" in Carrara marble (CM), Montesclaros marble (MM) and Redueña dolomite (RD). It can be seen that the roughness decreases with the pitch, in both holes and grooves; corresponding the maximum value to the lower pitch, 40 μm, given that increasing the separation between structures increases the surface that is not laser ablated. Moreover, values of the root mean square height, Sq, are higher for grooves than holes but diminish faster with the pitch in the case of holes than grooves. On the other hand, for the same pitch, CM and RD present higher roughness (above 5 μm) tan MM (≤5 μm). The same behaviour has been observed in the mean roughness, Sa, but with lower values than in Sq, because the latter is a more sensitive parameter than the arithmetic mean to large localized irregularities, as it is the case of the laser texturing regular patterns used in this work.

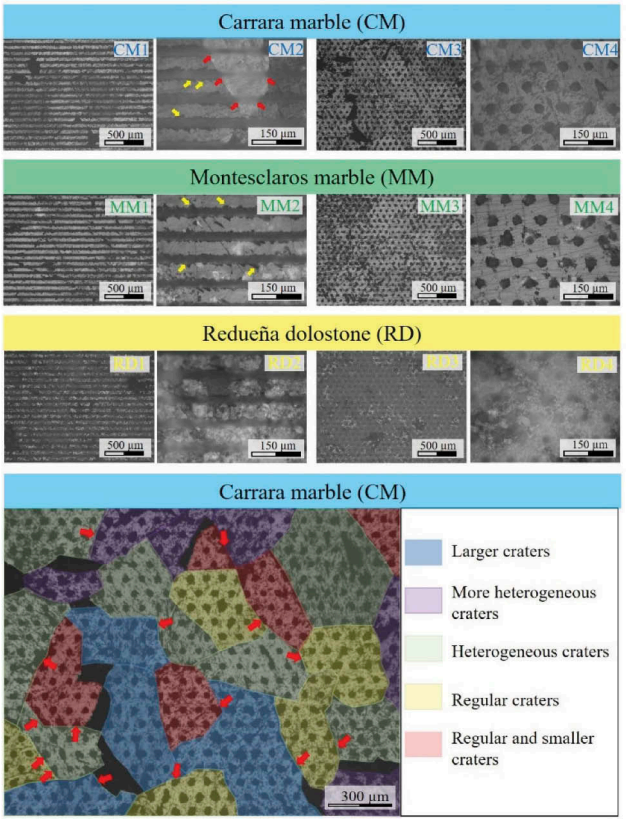

Figure 6. Bulk samples texturing (parallel grooves and hole matrix) of Carrara marble (CM), Montesclaros marble (MM) and Redueña dolomite (RD). Bottom figure: Enlargement of the MM3 bulk sample with the division of the calcite crystals according to the morphology of the craters.

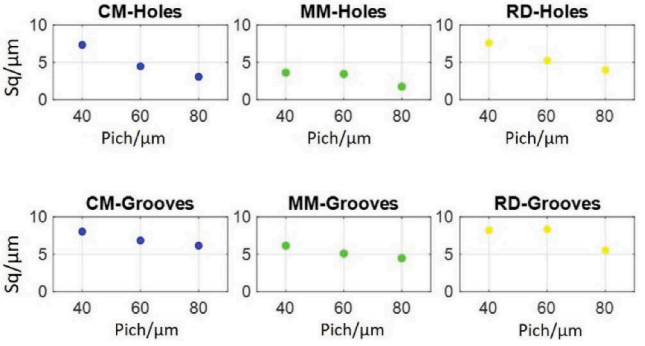

Figure 7. Root mean square height Sq vs. pitch, of the textured samples of Carrara marble (CM), Montesclaros marble (MM) and Redueña dolomite (RD).

To explain the different responses under femtosecond laser texturing of these carbonate stones; Carrara marble (CM), Montesclaros marble (MM) and Redueña dolostone (RD); the structure of calcite must be considered (Figure 8): A calcite crystal is shown in Figure 8a, and the acute rhombohedral unit cell of calcite indicating the cleavage rhombohedron setup in Figure 8b. The true unit cell includes 2 $CaCO_3$ with calcium ions at the corners of the

rhombohedrons and CO_3 groups, each of which consists of a carbon ion at the centre of a planar group of oxygen atoms whose centres define an equilateral triangle (Figure 8c). This atomic arrangement conditions the fracture produced by laser texturing in calcite crystals, especially when this calcite has not undergone a metamorphism process, as is the case with marbles. For this reason, the craters of the marbles show a more circular morphology than the craters produced in the neoformation calcite included in the fill of RD fossils. These craters are triangular (Figure 3 RD3), depending on the direction of incidence of the laser with respect to the structure of calcite.

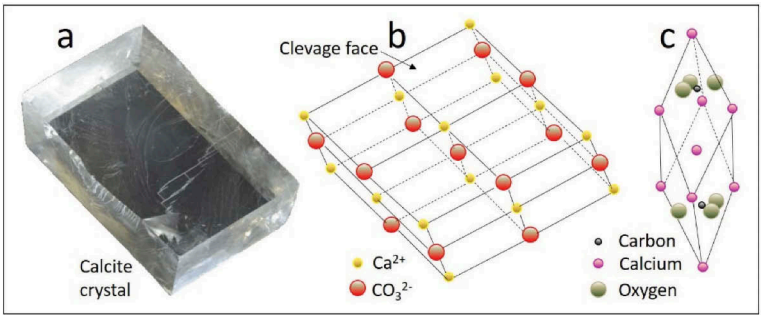

Figure 8. Calcite structure. a) Calcite crystal, b) Calcite unit cell, c) Atomic arrangement. Modified of Encyclopedia Britannica, 1994.

Crystal size and microcracks also influence crater morphology. In this sense, CM has crystal size of 300 μm and these crystals have intercrystalline microcracks. This disposition of the crystals generates more heterogeneous craters than MM (average crystal size of 1 mm), because there are more planes of weakness. The greater size of craters in the crystal boundaries is due to crater spreads along the crystal boundary. In addition, a greater deformation in this zone due to the grain boundary sliding must be considered (Hou et al., 2022). In the case of the micritic cement present in RD, its low crystallinity does not produce this effect, for this reason the craters appear circular and diffuse.

The combination of these characteristics means that, despite being three carbonate stones, their responses to laser texturing give different morphology of the generated structures and, consequently, different surface roughness (Figure 7). Moreover, with regards to the stones, CM and RD present values of Sq above 5 μm; while MM is always below this value. This indicates that a greater heterogeneity of the stones in terms of the type of calcite (RD), but also in terms of number of intercrystalline limits (CM), results in a greater surface roughness than in the case of stones like MM with large crystal size.

4 CONCLUSIONS

Calcite present in the marbles (CM and MM) has generated more regular craters than the neoformation calcite that fills the fossils in Redueña dolostone (RD). The craters generated in the neoformation calcite are more conditioned by microcracks due to the microstructure of the calcite. In the case of the micritic cement present in the RD, its low crystallinity does not produce this effect and the craters appear circular and with fuzzy edges. The differences observed in thin sections allowed us to understand the differences observed in laser-structured bulk samples and, specifically, in the roughness values achieved by each of the heritage calcareous stones as a function of the textured pattern. This is a crucial parameter when designing conservative strategies based on laser texturing.

Finally, policies to maintain and restore built heritage must be enacted in consultation with specialists in the science of stone conservation to follow an appropriate strategy for

preservation. European directives and the scientific community advocate preventive conservation rather than interventional conservation (UNESCO 2011). Therefore, the causes of building stone decay must be identified, and the means needed to mitigate them must be utilized.

ACKNOWLEDGMENTS

This work was supported by the Portuguese Foundation for Science and Technology (FCT) in the framework of the Strategic Funding, with UIDB/00073/2020 and CEECIND/03568/2017 projects. Authors acknowledge Erasmus+ program: HERDADE Consortium (2021-1-ES01-KA130-HED-360 000007519). This paper has been written during a scientific stay at the Centro de Ciencias Sociales y Humanas (CSIC) in Madrid within the framework of the project entitled: Use and function of the peninsular granary caves: an approximation based on archaeobotany (PID2021-127936NB-I00).

REFERENCES

Ariza R., Alvarez-Alegria, M., Costas, G., Tribaldo, L., R. Gonzalez-Elipe, A. & Siegel, J. 2022. Multiscale ultrafast laser texturing of marble for reduced surface wetting. *Applied Surface Science* 577: 151850. https://doi.org/10.1016/j.apsusc.2021.151850.

Carrascosa, L.A.M., Zarzuela, R., Botana-Galvín, M., Botana, F.J. & Mosquera, M.J. 2022. Achieving superhydrophobic surfaces with tunable roughness on building materials via nanosecond laser texturing of silane/siloxane coatings. *Journal of Building Engineering* 58: 104979. https://doi.org/10.1016/j.jobe.2022.104979.

Cassar J. 2010. The use of limestone in a historic context – the experience of Malta. *Geological Society, London, Special Publications* 331: 13–25. https://doi.org/10.1144/SP331.2.

De Wever, P., Baudin, F., Pereira, D., Cornée, A., Egoroff, G. & Page, K. 2017. The Importance of Geosites and Heritage Stones in Cities—a Review. *Geoheritage* 9: 561–75. https://doi.org/10.1007/s12371-016-0210-3.

Fehér, K. & Török, Á. 2022. Detecting short-term weathering of stone monuments by 3D laser scanning: lithology, wall orientation, material loss. *Journal of Cultural Heritage* 58:245–55. https://doi.org/10.1016/j.culher.2022.10.012.

Fiorucci, M.P., López, A.J. & Ramil, A. 2014. Comparative study of surface structuring of biometals by UV nanosecond Nd:YVO4 laser. The International Journal of Advanced Manufacturing 394 *Technology*; 75: 515–521. https://doi.org/10.1007/s00170-014-6164-1.

Fort, R., Alvarez de Buergo, M., Perez-Monserrat, E.M., Gomez-Heras, M., Jose Varas- Muriel, M. & Freire D.M. 2013. Evolution in the use of natural building stone in Madrid, Spain. *Quarterly Journal of Engineering Geology and Hydrogeology* 46:421–9. https://doi.org/10.1144/qjegh2012-041.

Freire-Lista, D.M. & Fort, R. 2017. Historical Quarries, Decay and Petrophysical Properties of Carbonate Stones Used in the Historical Center of Madrid (Spain). *AIMS Geosciences* 3:284–303. https://doi.org/10.3934/geosci.2017.2.284.

Freire-Lista, D.M. & Fort, R. 2019. Historical City Centres and Traditional Building Stones as Heritage: Barrio de las Letras, Madrid (Spain). *Geoheritage* 11: 71–85. https://doi.org/10.1007/s12371-018-0314-z.

Freire-Lista, D.M. 2020. Geotourism from fuente de cibeles of Madrid. History, building stones and quarries. *Cadernos Do Laboratorio Xeoloxico de Laxe* 42:69–94. https://doi.org/10.17979/CADLAXE.2020.42.0.7286.

Freire-Lista, D.M. 2021. The Forerunners on Heritage Stones Investigation: Historical Synthesis and Evolution. *Heritage*; 4:1228–68. https://doi.org/10.3390/heritage4030068.

Hou, C., Liu, J., Zheng, Y., Sun, Y., Zhou, B. & Fan, W. 2022. Prolonged grain boundary sliding in naturally deformed calcite marble at the middle crustal level. *Journal of Structural Geology* 161:104658. https://doi.org/10.1016/J.JSG.2022.104658.

Huerta-Murillo, D., García-Girón, A., Romano, J.M., Cardoso, J.T., Cordovilla, F., Walker, M., Dimov S.S. & Ocaña, J.L. 2019. Wettability modification of laser-fabricated hierarchical Surface structures in Ti-6Al-4V titanium alloy. *Applied Surface Science* 463:838–46. https://doi.org/10.1016/J.APSUSC.2018.09.012.

López, A.J., Ramil, A., Pozo-Antonio, J.S., Rivas, T. & Pereira, D. 2019. Ultrafast laser Surface texturing: A sustainable tool to modify wettability properties of marble. *Sustainability* 11: 4079. https://doi.org/10.3390/su11154079.

López, A.J., Pozo-Antonio, J.S., Moreno, A., Rivas, T., Pereira, D. & Ramil, A. 2022. Femtosecond laser texturing as a tool to increase the hydrophobicity of ornamental stone: The influence of lithology and texture. *Journal of Building Engineering* 51: 104176. https://doi.org/10.1016/j.jobe.2022.104176.

López de Azcona, M.C., Fort González, R. & Mingarro Martín, F. 2002. La conservación de los materiales pétreos en la Fuente de Cibeles, Madrid (España). *Materiales de Construcción* 52: 65–75. https://doi.org/10.3989/mc.2002.v52.i265.345.

Martínez-Martínez, J., Benavente, D. & García-del-Cura, M.A. 2011. Spatial attenuation: The most sensitive ultrasonic parameter for detecting petrographic features and decay processes in carbonate rocks. *Engineering Geology* 119: 84–95. https://doi.org/10.1016/j.enggeo.2011.02.002.

Murru, A., Freire-Lista, D.M., Fort, R., Varas-Muriel, M.J. & Meloni, P. 2018. Evaluation of post440 thermal shock effects in Carrara marble and Santa Caterina di Pittinuri limestone. *Construction and Building Materials* 186: 1200–1211. https://doi.org/10.1016/j.conbuildmat.2018.08.034.

Pou-Álvarez, P., Riveiro, A., Nóvoa, XR., Fernández-Arias, M., del Val, J., Comesaña, R., Boutinguiza, M., Lusquiños, F. & Pou, J. 2021. Nanosecond, picosecond and femtosecond laser surface treatment of magnesium alloy: role of pulse length. *Surface and Coatings Technology* 427:127802. https://doi.org/10.1016/j.surfcoat.

Salvini, S., Bertoncello, R., Coletti, C., Germinario, L., Maritan, L., Massironi, M., Pozzobon, R. & Mazzoli C. 2022. Recession rate of carbonate rocks used in cultural heritage: Textural control assessed by accelerated ageing tests. *Journal of Cultural Heritage* 57: 154–64. https://doi.org/10.1016/j.culher.2022.08.010.

Salvini, S., Coletti, C., Maritan, L., Massironi, M., Pieropan, A., Spiess, R. & Mazzoli, C. 2023. Petrographic characterization and durability of carbonate stones used in UNESCO World Heritage Sites in northeastern Italy. *Environmental Earth Sciences* 82: 49. https://doi.org/10.1007/s12665-022-10732-y.

Sanz, M., Oujja, M., Ascaso C., de los Ríos, A., Pérez-Ortega, S., Souza-Egipsy, V., Wierzchos, J., Speranza, M., Cañamares, M.V. & Castillejo M. 2015. Infrared and ultraviolet laser removal of crustose lichens on dolomite heritage stone. *Applied Surface Science* 346:248–55. https://doi.org/10.1016/j.apsusc.2015.04.013.

Siegesmund, S, Ullemeyer, K, Weiss, T & Tschegg, E.K. 2000. Physical weathering of marbles caused by anisotropic thermal expansion. *International Journal of Earth Sciences* 89:170–82. https://doi.org/10.1007/s005310050324.

Taelman, D, Delpino, C & Antonelli, F. 2019. Marble decoration of the Roman theatre of Urvinum Mataurense (Urbino, Marche region, Italy): An archaeological and archaeometric multi-method provenance study. *Journal of Cultural Heritage* 39: 238–50. https://doi.org/10.1016/j.culher.2019.03.009.

Weber, J, Beseler, S & Sterflinger, K. 2007. Thin-section microscopy of decayed crystalline marble from the garden sculptures of Schoenbrunn Palace in Vienna. *Materials Characterization* 58:1042–51. https://doi.org/10.1016/j.matchar.2007.04.014.